

An Efficient Adaptive Filtering for CFA Demosaicking

Dev. R. Newlin*, Elwin Chandra Monie**

* Vice Principal & Head Dept. of ECE, SATYAM College of Engineering & Technology, Aralvoimozhy

** Addl. Director, Department of Technical Education, Chennai.

*Mail ID: dev_r_newlin@yahoo.com

Abstract

Most digital still cameras acquire imagery with a color filter array (CFA), sampling only one color value for each pixel and interpolating the other two color values afterwards. The interpolation process is commonly known as demosaicking. In general, a good demosaicking method should preserve the high-frequency information of imagery as much as possible, since such information is essential for image visual quality. We discuss in this paper two key observations for preserving high-frequency information in CFA demosaicking: 1) the high frequencies are similar across three color components, and 2) the high frequencies along the horizontal and vertical axes are essential for image quality. Our frequency analysis of CFA samples indicates that filtering a CFA image can better preserve high frequencies than filtering each color component separately. This motivates us to design an efficient filter for estimating the luminance at green pixels of the CFA image and devise an adaptive filtering approach to estimate the luminance at red and blue pixels. Experimental results on simulated images, as well as raw data, verify that the proposed method outperforms the existing methods both visually and in terms of peak signal-to-noise ratio, at a notably lower computational cost.

Keywords-demosaicking, bilinear, luminance, spectrum

I. INTRODUCTION

To reduce cost and size, most digital still cameras (DSC) use a single electronic sensor covered with a color filter array (CFA) to acquire imagery, sampling only one color value for each pixel. To restore a full-color image from these CFA samples, the two missing color values at each pixel need to be estimated a process that is commonly referred to as demosaicking. Today, the most popular CFA pattern is Bayer pattern [1], a schematic of which is shown in Fig. 1, where green (G) values are sampled in a quincuncial lattice, while red (R) and blue (B) values are in two separate rectangular lattices. Estimating the missing color values is possible because of substantial correlation between neighboring pixel intensities (interpixel correlation).

Bilinear and bicubic demosaicking use isotropic neighborhoods, which may lead to over smoothing of edges. In real images, the interpixel correlations are anisotropic, i.e., the correlation is larger along the edges and smaller across the edges. Several researchers suggested using this property to improve the performance of demosaicking. The bilinear and bicubic interpolation techniques remove the aliasing by eliminating the overlapped high-frequency content. This elimination is similar to low-pass filtering [2], [3], which could degrade the quality of the resultant image, especially in the more sparsely sampled red and blue components. A good demosaicking method should remove the aliasing artifacts

while at the same time preserving as much high-frequency information as possible. To better preserve high-frequency information in demosaicking, the key is to exploit the strong correlations across color components (or planes). Our experimental results further confirm that the detail wavelet coefficients of three color planes are not only strong correlated, but also similar to each other [9]. This can explain why color-difference images are smooth and suitable for interpolation.

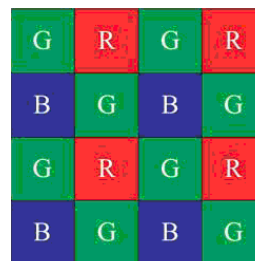


Fig.1. Bayer color filter array pattern.

The similarity also implies that in demosaicking we could reconstruct a full-resolution image plane containing the high-frequency information, and then use it to estimate the missing color values. An appropriately designed low-pass filter can be used to reconstruct from a CFA image a full-resolution luminance plane, which is then used as a reference to reconstruct the missing color values. However, the filter proposed in [8] unnecessarily eliminates high-frequency information along the horizontal and vertical axes, which is important for image quality, as we will demonstrate in Section II-B. Our frequency analysis of Bayer CFA samples indicates that the important high-frequency information along the two axes is preserved, free of aliasing, in the sub sampled green plane and, hence, can be extracted by a properly designed filter. Based on our analysis, we propose in Section III an efficient low-pass filter for luminance of green samples to better preserve the high-frequency information. The high-frequency information at red/blue pixels is then estimated by adaptive filtering of color-difference components (Section IV). Incorporating these techniques for preserving high-frequency information, our method outperforms existing state-of-the-art methods both visually and in terms of peak signal-to-noise ratio (PSNR).

II. KEY OBSERVATIONS ABOUT CFA DEMOSAICKING

In this section, we discuss two key observations that can help better preserve the high-frequency information in demosaicked images.

A. Similarity of Inter-color High-Frequency Content

Gunturk *et al.* have demonstrated that the high-frequency components of three color planes are highly correlated, with correlation values ranging from 0.98 to 1 [7]. Generally, a high correlation between two variables does not necessarily mean their equality. However, the smoothness of color-difference planes implies that the high-frequency components from different color components are not only correlated but also similar to each other [9]. This approximate equality of high-frequency information between color planes has been well exploited in demosaicking. The most popular way of exploiting this property is through interpolation of the color-difference images. For example, this can be done by estimating a full-resolution green component first and then using it to predict the red and blue components from color-difference images. The following lemma explains why this approach works.

Lemma 1: Let F be a full-resolution reference color component. Then any other full-resolution color component $C \in \{R,G,B\}$ can be predicted from its sub sampled version using

$$C \approx I(C_s - F_s) + F \quad (1)$$

where F_s is sub sampled version of F and I denotes a proper interpolation process.

B. Importance of Different High-Frequency Components

In natural images, the energy spectrum is primarily concentrated in a low-frequency region, along the horizontal and vertical axes. A typical example is shown in Fig. 2

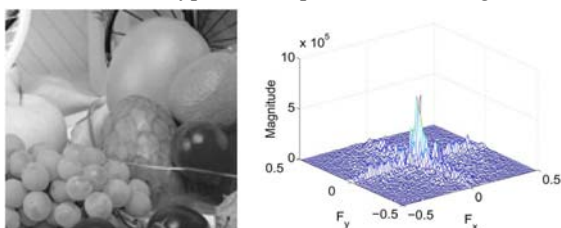


Fig. 2. (a) A test image and (b) its spectrum

To understand the importance of different high-frequency components, we removed from a set of images their high-frequency coefficients outside the central circle [see Fig. 3(a)], and outside a region more elongated along the two axes [see Fig. 3(b)], respectively, while preserving the same amount of image energy. We found that the latter results are generally more visually pleasing than the former, even though the preserved energy is the same. This experiment shows that high-frequency information along the horizontal and vertical axes has larger impact on the image quality than that at the corners. This is because the human visual system is more sensitive to the information of these high frequencies.

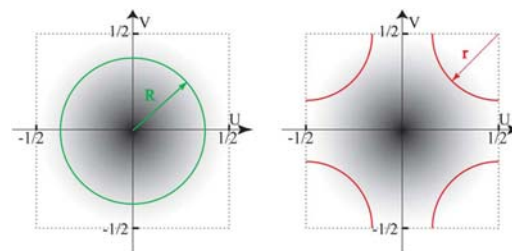


Fig. 3. Removing (a) frequency coefficients outside the central circle and (b) frequency coefficients outside a region elongated along both axes, respectively

III. BETTER LUMINANCE FILTERING AT GREEN SAMPLES

According to the CFA spectrum $A(u, v)$, the replicas of color-difference component in the horizontal and vertical directions have the same amplitudes but inverse signs. If we sub-sample CFA at only green-pixel locations, the side components in these two directions will overlap and cancel out each other

$$A(u, v) * D_G(u, v) = G_s(u, v) \quad (2)$$

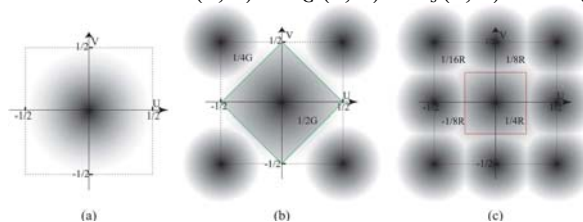


Fig. 4. Fourier transforms of (a) full-resolution color component, (b) quincuncially sampled green component, and (c) rectangularly sampled red/blue component.

The resultant spectrum has no replicas at the sides, as shown in Fig. 4(b). If we remove the corner components $C2$ before subsampling the CFA image, the resultant spectrum will coincide with the luminance spectrum. Specifically, let $A'(u, v)$ be the spectrum with the corner components $C2$ removed, then

$$A'(u, v) * D_G(u, v) = \frac{1}{4} [2G + R + B](u, v) * D_G(u, v) = L(u, v) * D_G(u, v) \quad (3)$$

The advantage of this approach is that the low-pass filter removing corner components $C2$ has a quincuncial shape and, hence, preserves the important high-frequency information along the horizontal and vertical axes. One example of such quincuncial filter is shown in Fig. 4(b), which is often used in bilinear interpolation. However, we can see that such a quincuncial filter yields poor performance because it also removes a part of component $C1$. This leads to much larger mean square error (MSE) of the estimated luminance. An alternative solution is to simply modify the Alleysson's filter with $r1 = 0$, as shown in Fig. 5(a). This substantially reduces the MSE, where we iteratively computed the optimal parameters to achieve the best MSE, as Alleysson *et al.* did [8]. Our Experimental results show that the optimal values of $r2$ are typical in a small range around [0.08, 0.16]. Moreover, the MSE degrades little around the optimal value. A larger filter size can reduce the MSE values more. The reduction becomes minimum when the filter size is larger than 5×5 . Hence, we fixed our filter size as 5×5 in order to

reduce the computational cost. The spectrum and the impulse response of the proposed 5 X 5 filter are shown in Fig. 5(b) and (c).

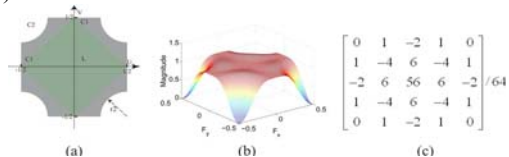


Fig. 5. Proposed low-pass filter for green pixel luminance: (a) passband, (b) spectrum, and (c) impulse response

Since the passband of the proposed filter is fixed, it does not depend on the image content. Despite this simplification, the performance of the redesigned filter only degrades slightly in terms of MSE. Computationally, it requires only five multiplications and 20 additions for each pixel, compared to 21 additions and 68 multiplications for the Alleysson's 11 X 11 filter. However, the proposed low-pass filter is not suitable for estimating the luminance at red/blue pixel locations, because the side replicas of the component do not cancel out at these locations. To address this problem we propose using an adaptive filtering scheme, as described in Section IV.

IV. ADAPTIVE LUMINANCE FILTERING AT RED/BLUE SAMPLES

According to Lemma 1, we can interpolate the estimated, sub-sampled version of luminance (at green-sample locations, see Section III) to full resolution by using the difference images $Cr = L - R$ [see Fig. 6(a)] or $Cb = L - B$. However, this is one type of a chicken-and-egg problem, as the references must have full resolution, which requires extension of sub-sampled red/blue components to full resolution. But, the red/blue components also require a full-resolution reference, such as the full-resolution luminance.

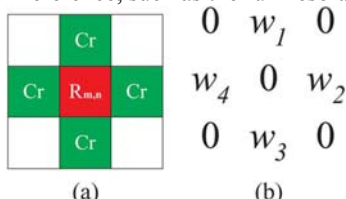


Fig. 6. (a) Reference neighboring samples and (b) the adaptive filter

We propose resolving this problem iteratively. We start with bilinear interpolation of red and blue components, separately; to full resolution, and then use these estimated components to interpolate a full-resolution version of the luminance (using Lemma 1). Hence, we improve the first estimates of full-resolution red and blue components by using the estimated luminance as a reference. This process can be repeated several times, until no further changes occur or the changes are sufficiently small. Our experiments show that two iterations are sufficient in most cases.

Since the first step, bilinear interpolation of red/blue components may fail to preserve high-frequency information $F_1 \approx F^l$, for $F \in \{R, B\}$, the high-frequency information will also be lost in the second step, bilinear interpolation of the luminance component.

According to Lemma 1,

$$\hat{L} = I_{bil}(L_s - F_s^l) + F^l \approx L^l \quad (4)$$

where I_{bil} designates bilinear interpolation. To better preserve the high-frequency information we propose using an anisotropic adaptive interpolation for the color-difference components.

We define the adaptive filter coefficients, w_k , $k=1$ to 4, shown in Fig. 6(b), to be proportional to the spatial correlation along the corresponding directions, which can adapt to different neighborhood spatial patterns. In our adaptive filtering, the correlations (and, hence, the coefficients) are estimated from the neighborhood pixel values.

For red-sample locations shown in Fig. 6(a), the coefficients are defined as

$$\begin{aligned} \frac{1}{w_1} &= 1 + |R(m, n) - R(m, n + 2)| + |L(m, n + 1) - L(m, n - 1)| \\ \frac{1}{w_2} &= 1 + |R(m, n) - R(m - 2, n)| + |L(m + 1, n) - L(m - 1, n)| \\ \frac{1}{w_3} &= 1 + |R(m, n) - R(m, n - 2)| + |L(m, n + 1) - L(m, n - 1)| \\ \frac{1}{w_4} &= 1 + |R(m, n) - R(m + 2, n)| + |L(m + 1, n) - L(m - 1, n)| \end{aligned} \quad (5)$$

Note that these expressions define a type of edge detector; the presence of edge makes the corresponding coefficients small. Not only does the edge detector operate directly on the subsampled data, it can also work on diagonal edges. Similar weights can be used for interpolation at blue-sample locations.

Iterating the adaptive filtering can improve the performance of luminance estimation, especially in the first two iterations. More iteration, however, may negate the improvement. The negation happens because the equivalent filter size after several iterations becomes very large and may involve many pixels that are only slightly correlated. To avoid performance degradation and minimize the computation, we, therefore, perform two iterations in the proposed red/blue-sample luminance estimation. Overall, the proposed approach has a notably better performance (in terms of MSE) compared with the Alleysson's filter.

V. EXPERIMENTAL RESULTS

To evaluate the proposed method we compare it with five demosaicking techniques

- Alternating projections (AP) [7]
- Successive approximation (SA) [6]
- Primary-consistent soft-decision (PCSD) [4],
- Frequency selection (FS) [8]
- Adaptive homogeneity-directed demosaicking [5]
- Bilinear interpolation

Among these methods, bilinear interpolation is the simplest and also most common reference for performance comparison in the demosaicking literature. The AP method projects the high frequencies of green component to red and blue components, the SA method iterates its isotropic interpolation, and the FS method selectively filters CFA image to estimate the luminance. These three methods are not anisotropic. On the other hand, the PCSD's anisotropic interpolation criterion is obtained from training, and AHD's is

based on some homogeneity similarity measure. The PSNR results obtained by the methods under comparison are summarized in Table I.

TABLE 1 PSNR PERFORMANCE (IN DECIBELS) COMPARISON FOR EACH TEST IMAGE FOR RED, GREEN, BLUE PLANES

Image		Bilinear	AP	PCSD	SA	FS	AHD	Proposed
1	R	25.31	36.59	36.35	36.66	35.06	34.62	36.68
	G	29.58	40.49	38.85	40.88	39.64	36.28	39.92
	B	25.35	36.86	36.55	37.64	35.45	34.79	36.90
2	R	31.89	35.87	37.32	35.54	34.04	36.59	37.71
	G	36.26	40.81	42.59	40.06	39.70	41.56	43.71
	B	32.36	38.60	40.78	39.07	36.57	40.19	40.10
3	R	33.45	40.43	41.46	39.08	38.68	40.64	42.19
	G	37.17	43.48	44.67	42.21	42.20	43.74	45.63
	B	33.83	40.39	40.88	39.36	38.49	40.16	41.41
4	R	32.61	36.68	36.31	36.17	35.21	35.74	37.16
	G	36.53	43.33	43.31	42.64	42.99	41.74	44.67
	B	32.91	41.42	42.18	40.88	40.76	40.98	42.63
5	R	25.75	36.82	36.73	35.59	34.97	35.14	37.51
	G	29.32	39.81	39.80	38.27	38.27	37.46	40.84
	B	29.92	36.55	36.14	35.34	34.80	34.44	36.86
6	R	26.70	37.72	39.32	37.22	36.25	37.60	37.70
	G	31.05	41.52	41.49	41.40	40.81	39.13	40.74
	B	27.00	37.27	37.99	36.67	35.67	36.51	36.85
7	R	32.57	40.84	41.02	40.12	38.89	40.12	42.27
	G	36.47	43.62	43.76	42.67	42.44	42.71	45.61
	B	32.58	39.91	39.82	39.35	38.08	39.08	40.93
8	R	31.05	35.37	36.28	35.34	34.85	35.52	40.08
	G	35.36	39.02	40.05	39.58	39.56	40.69	41.47
	B	32.26	36.79	39.67	38.83	37.45	38.61	39.94

Our method outperforms the other methods for the overwhelming majority of test images. On average, the improvement to bilinear is quite large, up to 8.8 dB. The improvement to the AP, PCSD and SA methods is around 0.5 dB–1.0 dB, and that to the FS and AHD methods is around 1.5 dB–2.3 dB. Consistent performance improvement can be obtained when using S-CIELAB [12], [13]. The proposed method produces visually favorable results with sharper edges compared to most other methods. Our method obtains the best perceptual results with sharper edges and fewer zipper artifacts. Bilinear interpolation yields blurred edges and many color artifacts. The AP, SA, and FS methods produce severe zipper artifacts around the edges due to the use of isotropic interpolation. The PCSD method can obtain better results since it uses an anisotropic interpolation technique, but the training criterion it uses for edge direction estimation may be inaccurate for some image regions, leading to some artifacts. As reported in Gunturk’s review paper [10], the AHD method can produce perceptually favorable images with fewer artifacts. The approach uses a type of anisotropic filtering, based on some homogeneity criteria for neighborhood similarity.

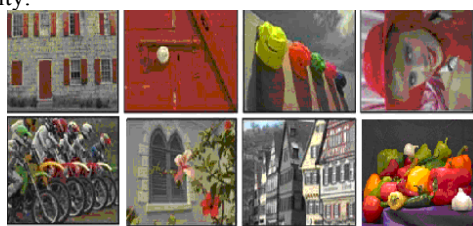


Fig. 7. Test Images (referred as Image 1 to 8)

However, the interpolation is restricted to one of two directions (horizontal or vertical), which may not work well for textured images, where high-frequency components might

need to be preserved in both directions. Our method can better preserve the textured structures due to the adopted adaptive filtering. Our method yields better PSNR performance (see Table I), and has much lower computational cost.

VI. CONCLUSION

In this paper, we have discussed two important observations for preserving high-frequency information in CFA demosaicking. First, we have shown that due to the similarity of high-frequency information across three color components, one full-resolution component can be used to estimate the high-frequency information of all other components. We have also shown that high-frequency information along horizontal and vertical axes is more important for image quality than that in the spectrum’s corners. Our frequency analysis explains why the Bayer CFA pattern can preserve the vital high-frequency information.

Based on these observations, we propose an adaptive filtering demosaicking method for better preservation of high-frequency information. We designed an efficient low-pass filter on CFA image to estimate the luminance at green-sample locations. The proposed filter can preserve more high frequencies than the existing filters. Next, an adaptive filtering is used to estimate the luminance at red and blue samples. Our frequency analysis indicates that the proposed adaptive filter is well suited for varying image content and can better preserve high frequencies. Experimental results confirm that the proposed method outperforms the existing state-of-the-art methods both visually and in terms of peak signal-to-noise ratio (PSNR), at a notably lower computational cost.

In CFA demosaicking, anisotropic techniques are usually required to preserve high frequencies around edges and remove zipper artifacts, but they incur high computational cost. Our analysis and proposed method show that a properly designed 5 X 5 filter can preserve well the high frequencies at green sample locations, without incurring much computational cost. Furthermore, our proposed adaptive filtering interpolation at red/blue sample locations can handle the diagonal edges more effectively than many existing anisotropic techniques do, leading to a better perceptual performance.

REFERENCES

- [1] B. Bayer, “Color imaging array,” U.S. Patent 3 977 065, 1976.
- [2] D. Cok, “Signal Processing method and apparatus for producing interpolated chrominance values in a sampled color image signal,” U.S. Patent 4 642 678, 1987.
- [3] J. Adams, “Interactions between color plane interpolation and other image processing functions in electronic photography,” in *Proc. SPIE Cameras and Systems for Electronic Photography and Scientific Imaging*, 1995, vol. 2416, pp. 144–151.
- [4] X. Wu and N. Zhang, “Primary-consistent soft-decision color demosaicking for digital cameras,” *IEEE Trans. Image Process.*, vol. 13, no. 9, pp. 1263–1274, Sep. 2004.
- [5] K. Hirakawa and T. W. Parks, “Adaptive homogeneity-directed demosaicking algorithm,” *IEEE Trans. Image Process.*, vol. 14, no. 3, pp. 360–369, Mar. 2005.
- [6] X. Li, “Demosaicking by successive approximation,” *IEEE Trans. Image Process.*, vol. 14, no. 3, pp. 370–379, Mar. 2005.

- [7] B. K. Gunturk, Y. Altunbasak, and R. M. Mersereau, "Color plane interpolation using alternating projections," *IEEE Trans. Image Process.*, vol. 11, no. 9, pp. 997–1013, Sep. 2002.
- [8] D. Alleysson, S. Susstrunk, and J. Herault, "Linear demosaicking inspired by human visual system," *IEEE Trans. Image Process.*, vol. 14, no. 4, pp. 439–449, Apr. 2005.
- [9] N.-X. Lian, V. Zagorodnov, and Y.-P. Tan, "Edge-preserving image denoising via optimal color space projection," *IEEE Trans. Image Process.*, vol. 15, no. 9, pp. 2575–2587, Sep. 2006.
- [10] B. K. Gunturk, J. W. Glotzbach, Y. Altunbasak, R. W. Schafer, and R.M. Mersereau, "Demosaicking: Color filter array interpolation," *IEEE Signal Process. Mag.*, vol. 22, no. 1, pp. 44–54, Jan. 2005.
- [11] L. Chang and Y. P. Tan, "Effective use of spatial and spectral correlations for color filter array demosaicking," *IEEE Trans. Consum. Electron.*, vol. 50, pp. 355–365, Feb. 2004.
- [12] W. Lu and Y.-P. Tan, "Color filter array demosaicking: New method and performance measures," *IEEE Trans. Image Process.*, vol. 12, no.10, pp. 1194–1210, Oct. 2003.
- [13] X. Zhang, S- Cielab: A Spatial Extension to the CIE LAB Delta E Color Difference Metric 1998 [Online]. Available: <http://white.stanford.edu/html/xmei/scielab/scielab.html>.